

# Photo-Removal of RB5 from Textile Industrial Waste by Zn (II) Complex Nano-Powder

Omima M. I. Adly<sup>1\*</sup> and M.S.A. Hussien<sup>1,2</sup>

<sup>1</sup>Department of Chemistry, Faculty of Education, Ain Shams University, Roxy, 11757 Cairo, Egypt.

<sup>2</sup>Nanoscience Laboratory for Environmental and Bio-medical Applications (NLEBA), Faculty of Education, Ain Shams University, Roxy, 11757 Cairo, Egypt.

Received: 22 Nov. 2017, Revised: 4 Dec. 2017, Accepted: 11 Dec. 2017.

Published online: 1 Jan. 2018.

**Abstract:** Zn(II) complex was prepared of hydrazone, H<sub>3</sub>L, ligand derived from the condensation of S-methylthiocarbamate and 4,6-diacetylresorcinol, in the molar ratio 1:1, has been synthesized. Zn(II) complex is dimmer. All the samples were characterized. These composites were applied for photo-irradiation of Reactive Black 5 (RB5) textile dye from textile industrial waste water under several conditions.

**Keywords:** Zn-complex, nano-composite; Photocatalytic activity; X-ray diffraction analysis; Transmission Electron microscope.

## 1 Introduction

Environmental pollution has become one of the demanding challenges to the sustainable improvement of modern human society, owing to industrialization, population growth and urbanization. We must use unlimited and sustainable energy influx from the Sun to the photo catalysis using solar energy because it was recognized as one of the most advantageous strategies to eliminate organic pollutants for relieving and resolving environmental issues facing mankind [1]. For the efficient utilization of sunlight, the development of visible-light-responsive photo catalyst is of great significance. Many metal oxides and sulfides such as WO<sub>3</sub> [2], CdS [3] and ZnS [4] can respond to visible light because the band gaps of these materials are generally narrower than those of TiO<sub>2</sub>, which is only photoactive under ultraviolet (UV) light [5]. Semiconductor nanostructures are ideal systems for exploring a large number of novel phenomena at the nanoscale and investigating the size and dimensionality dependence of their properties and potential applications [6]. ZnO oxide (ZnO) is an important oxide material with a wide direct band-gap (3.3eV), n-type semiconducting properties, with binding energy (60meV), has been extensively studied due to its potential applications [7,9]. In addition, ZnO is one of the ideal photo catalyst due to the low cost, nontoxic, and the photo generated holes with high oxidizing power for the degradation of environment

pollutants [10,12]. There are two major reasons to reduce the photo catalytic efficiency of ZnO. First, ZnO exhibits innately limited photoconversion performance under solar irradiation, which is attributed to its wide band gap and only allowed light absorption in the UV region [13]. Second, ZnO is also revealed the fast recombination of the photo generated electron-hole pairs to obstruct commercialization of the photocatalytic degradation process [14].

Metal-organic frameworks (MOFs), constructed from metal clusters interconnected by polydentate organic linkers, are a class of newly developed crystalline hybrid porous materials [15]. Their diverse structure features, such as large specific surface areas, uniform but tunable cavities and easily tailored chemistry, have endowed them with outstanding properties and potential applications in molecular sensing [16], gas storage [17], separation [18], and catalysis [19]. Unfortunately, the relatively fast recombination of photogenerated electrons and holes leads to unsatisfactory photo catalytic efficiencies of the reported MOFs [20]. To date, many attempts have been paid to enhance the photo catalytic performance of photo catalysts by suppressing electron-hole recombination, such as doping and surface modification [21]. Among them, modification of single photocatalyst materials with metal or metal oxide nano particles (mostly noble metal or metal oxide) to form metal/MOFs hetero-structured photo catalysts is a popular strategy [22,23], but the inevitable disadvantages of high

\* Corresponding author E-mail: [omima\\_adly@yahoo.com](mailto:omima_adly@yahoo.com)

price and limited abundance of noble metal restrict its practical application [20]. Alternatively, another important and feasible strategy to reduce charge carrier recombination probability is the addition of oxidants such as hydrogen peroxide ( $H_2O_2$ ), per sulfate (PS) and peroxymonosulfate (PMS) as electron acceptors to the photocatalytic reaction, owing to the immediate trapping of photo generated electrons by the oxidants [24,26]. The work from Du et al. [27] was one of few attempts to introduce external electron acceptors to the MOF-based photo catalysis system, which confirmed that ammonium per sulfate ( $(NH_4)_2S_2O_8$ ) could be used as an efficient oxidant to enhance the photo catalytic property of MOF photo catalyst for the depolarization of methylene blue (MB) under UV or visible light irradiation. However,  $(NH_4)_2S_2O_8$  is rather unstable in the photo catalytic process and the detailed mechanism of their action is not clarified. Ai et al. [28] found that the introduced  $H_2O_2$  could increase the photo catalytic activity of MOF.

In this study, Zn- complex [29] was in situ wrapped in nanopowders via a simple and facile preparation method from a single precursor solution of Zinc(II) nitrate hex hydrate. Photo catalytic properties of the prepared complex were investigated by photo degradation of RB5 under UV-light irradiation through different conditions. Furthermore, the factors influencing photo catalytic activity, the photo stability and the possible mechanism for the improved performance were also discussed.

## 2 Experimental

### 2.1 Synthesis of Zn- Complex

Zinc (II) nitrate hex hydrate,  $Zn(NO_3)_2 \cdot 6H_2O$ , (0.891 g, 3.0 mmol) in methanol (30 mL) was added gradually with constant stirring to a solution of the deprotonated, H<sub>3</sub>L, ligand (0.894 g, 3.0 mmol) in methanol (30 mL). The stoichiometry of the metal ion to ligand was 1:1. The solution was heated to reflux for three hours. A yellow precipitate was formed on cold and washed with small portions of methanol then ether. The yield was 1.68 g (68%) and the melting point was over 320°C (Figure 1) [29].

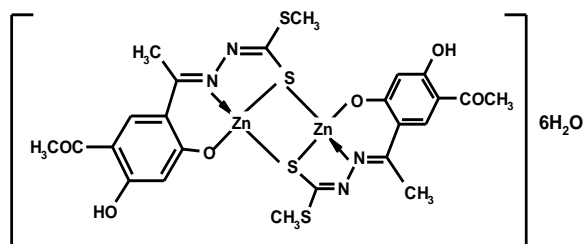


Figure 1. Structures of Zn(II) complex

### 2.2 Characterization of the Prepared Samples

The morphology of nanostructures was examined with a field emission scanning electron microscope (SEM) using a JEOL JSM-6500F SEM operating at 10 kV accelerating voltage. A JEOL-2010 transmission electron microscope (TEM) operating at 200 kV was used to examine the microstructures. The crystalline phase of the nanostructures was determined using the X-ray powder diffraction method (Shimadzu XRD-6000, CuK $\alpha$ 1 radiation ( $1 \frac{1}{4}$  0.1505 nm)). The cathode luminescence (CL) spectra were acquired with an electron probe micro analyzer (Shimadzu EPMA-1500) attached to a TEM. CL spectra were accumulated in a single shot mode within an exposure rate of 1 nm/s. All the CL spectra were taken at room temperature. The degradation of Reactive Black 5 (RB5) solution was used to evaluate the photocatalytic activity of Zn-complex nanoparticles. The RB5 solution was exposed to a 6 W UV lamp. For the photo catalytic activity evaluation, the concentration of photodegraded RB5 solution was recorded by a Hitachi U-2900 UV-vis spectroscopy.

### 2.3 Photocatalytic Activity

All experiments are proceeded in a 200ml thermostatic batch glass reactor as in our previous work [30], equipped with a magnetic stirrer. The photo-reactor consists of 8 xenon lamps each one has 254 nm wavelength of 6 watt. To 200 ml of the solution, to be investigated which could be phenol of different concentrations or with proper catalyst, were added and the resulting solution was subjected to UV irradiation within the photo reactor where a total radiant flux of 20 MWcm<sup>2</sup> was applied. The radiation flux was measured by a UV radiometer (Digital, UVX, 36). The aqueous suspension was magnetically stirred throughout the experiment. At different time intervals, aliquot was withdrawn which was subsequently filtered through 0.45 $\mu$ m (Millipore) syringe filter. The collected aliquots were then analyzed using UV-Vis Spectrophotometer.

## 3 Results and Discussion

### 3.1 Photocatalyst Characterization

#### 3.1.1 XRD

The crystal structure and orientation of Zn- Dar complex nanopowder arrays and nonmaterial arrays are investigated by XRD diffraction in Figure 2. The sharp diffraction peaks suggest that the as-synthesized nanostructures have a highly crystalline nature. Moreover, there is no diffraction peak corresponding to any clusters, which demonstrates that the as-synthesized nanostructures have high purity. The average nanocrystallite size ( $D$ ) of the Zn-Dar complex nanostructures was estimated using the Debye-Scherrer formula ( $D = 0.89 \lambda / \beta \cos \theta$ , where  $\lambda$  is the wavelength of

the Cu K  $\alpha$  irradiation,  $\beta$  is the FWHM of the diffraction peak, and  $\theta$  is the diffraction angle of the (002) planes of cubic Zn-Dar complex ) to be  $\sim 49.5$  nm. For the Zn-Dar complex nanostructures, all the diffraction peaks can be perfectly indexed to the pure cubic phase of Zinc bis(2-aminobenzoate) dehydrate ( $C_{14}H_{12}N_2O_4Zn \cdot 2H_2O$ ) (JCPDS no. 00-040-1617). The presence of this phase may lead to increase the photo catalytic activity of the prepared sample as the presence of the OH<sup>-</sup> enhances the behavior of the materials towards the degradation.

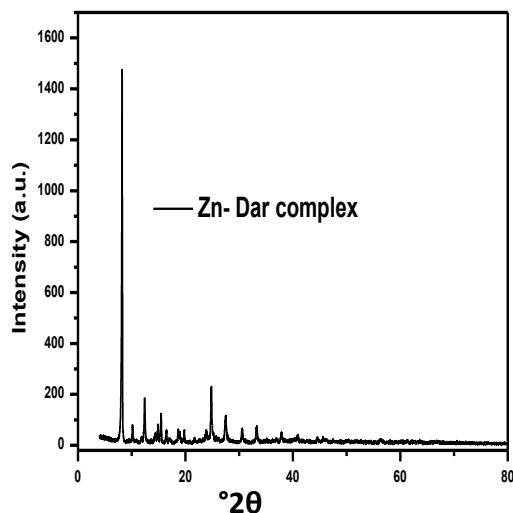


**Figure 2.**XRD pattern of Zn(II) complex

### 3.1.2 TEM

Detailed information on the assembled Zn(II) complex pseudo-spherical can be obtained by TEM (Figure 3). It can be seen that the bundled nanopseudo-spherical samples are really composed of chains, which are made up of one-dimensionally assembled nanoparticles with diameters ranged from 12 to 32 nm. Such a synthesis is interesting because though the synthesis of spherical - like nanopowder are composed of orderly assembled particles is rather uncommon with lots applications [31,32]. It can be envisioned that such ZnO powders may cherish the merits of both high specific area and structural stability, the hierarchically nanostructure spherical-like nanopowders are expected to be potential candidates for the catalysis based applications, where the assembled crystals may provide a significant enhance of effective electrode surface in comparison with its flower-like solid counterpart [33].

## 3.2 Photocatalytic Activity Results

### 3.2.1 RB5 Photo Stability

RB5 shows absorption peaks at 318, 390, 445 and 588 nm in Visible and UV regions respectively as shown in Figure 4. The rate of decolorization was recorded with respect to the change in intensity of the absorption peak at 588 nm. The absorption peaks, corresponding to dyes did not diminish during reaction, which indicated that the dyes had a marked stability towards degradation.

### 3.2.2 Effect of Zn- Complex Concentration

The effect of concentration of Zn-complex on photo catalytic degradation of RB5 dye have been investigated by Applying different concentrations of Zn-complex catalyst in photo degradation process as follows (0.025, 0.05, 0.0). The data represented in Figure 5 illustrate that, when wt of the Zn-complex is 0.025 gm, 90% of RB5 dye have been removed within 210min. However, upon increasing the percentage of Zn-complex concentration to 0.1 almost 100% degradation has been achieved. The data indicates also that the reaction rates are very fast during the first 50 min and decrease gradually with time; this may be due to the concentration of .OH which is very high at the start of reaction leading to the initial increase of degradation rate .Further, upon consumption of .OH radicals, the rate of degradation decreases gradually to reach a steady state at 150 min with 0.05gm Zn-complex. However, with 0.075 gm and 0.1gm Zn-complex a lowering in the reaction time was observed at 75 min. However, the rate of degradation started fast and decreased with time and become steady from 50-210min. This finding may be due to the consumption of .OH radicals by the RB5 molecules at longer times.

### 3.2.3 Effect of PH

One important feature in the photo degradation reaction is the pH change which should either be followed up during the reaction or adjusted at different values to evaluate the effect of its change on the degradation process.

#### 3.2.3.1 PH Change during the Degradation

In all experiments of RB5 dye degradation, the pH was monitored under all conditions. These results are shown in Figure 6. The variation of pH of the solutions occurs when the degradation process takes place and can be used as an evidence for the Commence of degradation. For example, during the degradation of RB5 dye ( $10^{-4}$  M) solution using different concentrations of Zn-complex catalyst the pH was found to decrease from 6.66 to 5.21 at room temperature upon exposure to UV irradiation this behavior may be due to the formation of some intermediates with acidic properties.

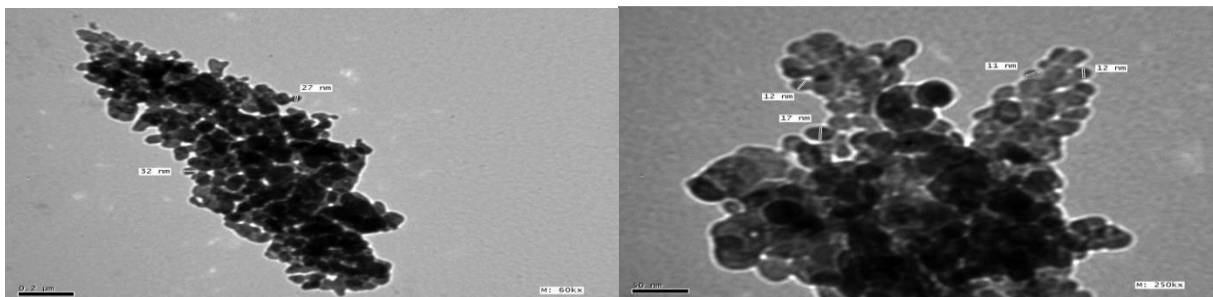


Figure 3. TEM image of Zn complex

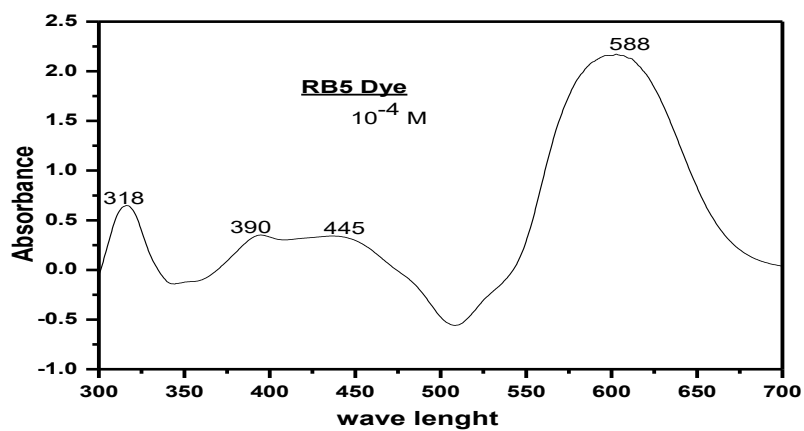


Figure 4. UV-VIS spectra of RB5 dye

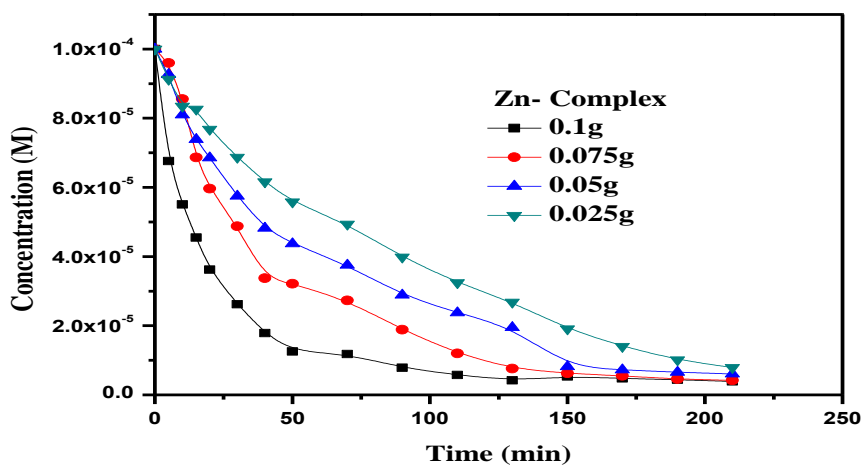
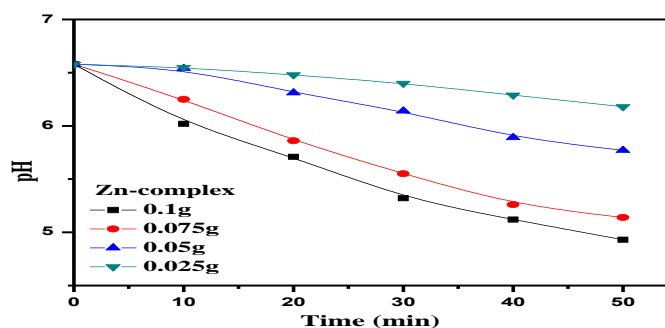


Figure 5. Effect of Zn-complex concentration on the photo catalytic degradation of RB5 dye



**Figure 6.** Variation of pH during the degradation of RB5 dye using different concentrations of Zn-complex

### 3.2.3.2 Effect of PH on the Degradation of RB5 Dye

Wastewater containing dyes is discharged at different pH; therefore, it is important to study the role of pH on decolorization of dye. To study the effect of pH on the decolorization efficiency, experiments were carried out at various pH values, ranging from 2 to 10 at a constant RB5 dye concentration ( $10^{-4}$  M) and catalyst dose (0.1 g/200mL), respectively. Figure 7 show the relation between concentration of RB5 dye solution and time on changing pH. It has been observed that the decolorization efficiency decreases with increase in pH exhibiting maximum rate of degradation at pH 6 for 0.1 gm Zn-complex. Similar behavior has also been reported for the photocatalytic decolorization of azo dyes [34]. The interpretation of pH effects on the efficiency of the photo catalytic degradation process is not straight forward because of its multiple effects. First, it is related to the acid base property of the metal complex surface. The adsorption of water molecules at surficial metal sites is followed by the dissociation of  $\text{OH}^-$  charge groups leading to coverage with chemically equivalent metal hydroxyl groups (M-OH) [35]. Due to amphoteric behavior of most metal hydroxides, the following two equilibrium reactions are considered [Eqs. (1) and (2)]



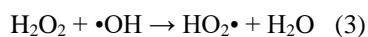
The presence of large quantities of  $\text{OH}^-$  ions on the particle surface as well as in the reaction medium favors the

formation of  $\text{OH}^\bullet$  radical, which is widely accepted as Principal oxidizing species responsible for decolonization process at acidic pH level and results in enhancement of the efficiency of the process [36].

The experimental results revealed that higher degradation of the dyes occurred in acidic region than in case of basic region. For Zn-complex, the rate of photodecolorization decreases with the increase in pH, exhibiting a maximum efficiency (95 %) at pH 2 after 160 min from the start of irradiation, beyond which the rate of degradation remained constant. This may be attributed to the electrostatic interactions between the positive catalyst surface and dye anions.

### 3.2.3.3 Effect of $\text{H}_2\text{O}_2$ as AOxidant in the Photo Degradation of RB5

The photocatalytic degradation of RB5 dye has been studied at different hydrogen peroxide concentrations and the results are illustrated in Figure 8. The degradation rate of RB5 dye increases with increasing  $\text{H}_2\text{O}_2$  concentration. The higher reaction rates after the addition of peroxide are attributed to the increase in the concentration of hydroxyl radical. According to Eq. (3), Hydrogen peroxide may split photocatalytically to produce hydroxyl radical directly, as cited in the studies of homogeneous photo-oxidation using  $\text{UV}/\text{H}_2\text{O}_2$  [34, 37].



Therefore, the proper addition of hydrogen peroxide can accelerate the photo degradation rate of RB5 dye. However, to keep the efficiency of the added hydrogen peroxide, it is necessary to choose the proper dosage of hydrogen peroxide, according to the kinds and concentrations of pollutants.

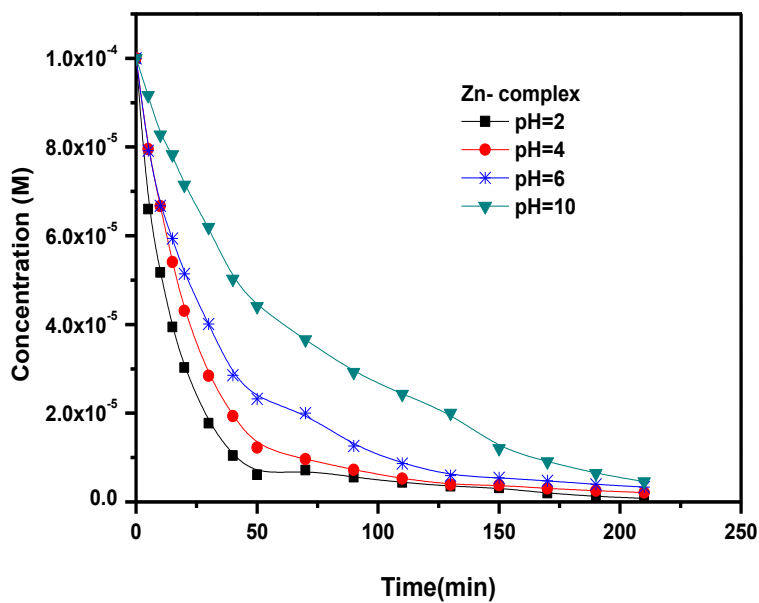


Figure 7. Photo degradation of LBR ( $10^{-4}$ M) at different pH (2, 4, 6 and 10) in presence of 0.1 g of Zn-complex

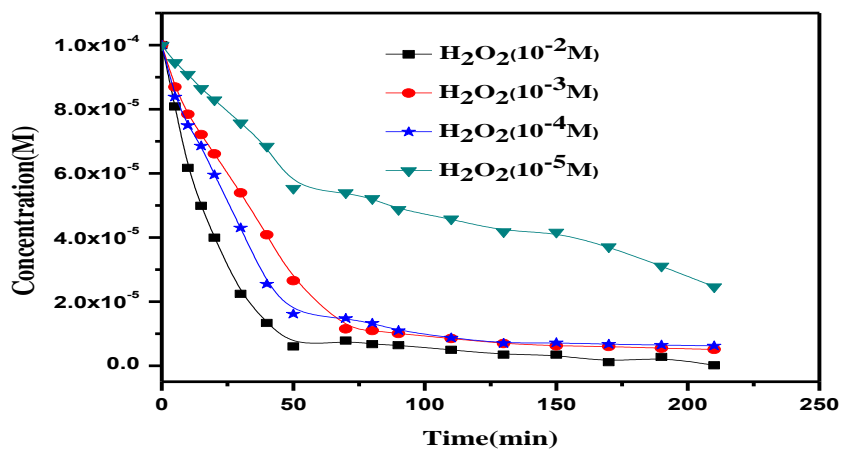


Figure 8. Degradation of ( $10^{-4}$ M) RB5 dye versus time at different concentrations of  $H_2O_2$

## 4 Conclusion

The experimental results revealed that 0.1gm of Zn-Dar complex was sufficient for the photodegradation of 200ml  $10^{-5}$  M RB5 textile dye. The rate of photodecolorization decreases with the increase in pH, exhibiting a maximum efficiency (95 %) at pH 2. The proper addition of hydrogen peroxide can accelerate the photo degradation rate of RB5 textile dye.

## Funding

This work is funded by a grant from Ain Shams University in the framework of projects of the scientific research.

## References

- [1] T. Zhang, W. Lin, *Chem. Soc. Rev.*; (2014),**43**, 5982–5993.
- [2] K. Villa, S. Murcia-López, T. Andreu and J.R. Morante, *Appl. Catal. B: Environ.* (2015),**163**,150–155.
- [3] S. Cao, C.J. Wang, X.J. Lv, Y. Chen and W.F. Fu, *Appl. Catal. B: Environ.* (2015),**162**, 381–391.
- [4] T. Baran, S. Wojtyła, A. Dibenedetto, M. Aresta and W. Macyk, *Appl. Catal. B: Environ.*(2015),**178**, 170–176
- [5] Yaowen Gao , Simiao Li , Yi xi Li , Linyu Yao , Hui Zhang *Applied Catalysis B: Environmental* 202 (2017) 165–174
- [6] X. Fang, Y. Bando, U.K. Gautam, C. Ye and D. Golberg, Inorganic semiconductor nanostructures and their field-emission applications, *J. Mater. Chem.* (2008),**18**, 509 - 522.
- [7] X. Zhang, X. Huang, C. Li and H. Jiang; Dye-sensitized solar cell with energy storage function through PVDF/ZnO nanocomposite counter electrode, *Adv.Mater.* (2013),**25**, 4093-4096.
- [8] I. Udom, M.K. Ram, E.K. Stefanakos, A.F. Hepp and D.Y. Go swami, Onedimensional-ZnO nanostructures: synthesis, properties and environmental applications, *Mater. Sci. Semicond. Process.* (2013),**16**, 2070e2083.
- [9] X. Tang, G. Li and S. Zhou, Ultraviolet electroluminescence of light-emitting diodes based on single n-ZnO/p-AlGa N-heterojunction nanowires, *Nano Lett.* (2013),**13**,5046-5050.
- [10] S. Senapati, S.K. Srivastava and S.B. Singh; Synthesis, characterization and photocatalytic activity of magnetically separable hexagonal Ni/ZnO nanostructure, *Nanoscale* (2012),**4**, 6604-6612.
- [11] F.-H. Chu, C.-W. Huang, C.-L. Hsin, C.-W. Wang, S.-Y. Yu, P.-H. Yeh, W.-W. Wu, and Well-aligned; ZnO nanowires with excellent field emission and photocatalytic properties, *Nanoscale*, (2012),**4**,1471-1475.
- [12] Z. Pei, L. Ding, M. Lu, Z. Fan, S. Weng, J. Hu, and P. Liu, Synergistic effect in Polyaniline-hybrid defective ZnO with enhanced photocatalytic activity and stability, *J. Phys. Chem. C*; (2014),**118**, 9570-9577.
- [13] Y.-H. Lu, W.-H. Lin, C.-Y. Yang, Y.-H. Chiu, Y.-C. Pu, M.-H. Lee, Y.-C. Tseng and Y.-J. Hsu.; A facile green antisolvent approach to Cu<sup>2+</sup>-doped ZnO nanocrystals with visible-light-responsive photo activities, *Nanoscale* (2014),**6**,8796-8803.
- [14] M.R. Hoffmann, S.T. Martin, W. Choi and D.W. Bahnemann; Environmental applications of semiconductor photocatalysis, *Chem. Rev.* (1995) **95**, 69-96.
- [15] D. Wang, R. Huang, W. Liu, D. Sun and Z. Li.; *ACS Catal.* (2014) **4**, 4254–4260.
- [16] Y. Bai, G.J. He, Y.G. Zhao, C.Y. Duan, D.B. Dang and Q.J. Meng.; *Chem. Commun.* (2006)**14**, 1530–1532.
- [17] L.J. Murray, M. Dinc̃a and J.R. Long.; *Chem. Soc. Rev.* (2009)**38**, 1294–1314.
- [18] L.J. Rong, R.J. Kuppler and Z.H. Cai.; *Chem. Soc. Rev.* (2009) **38**, 1477–1504.
- [19] J. Lee, O.K. Farha, J. Roberts, K.A. Scheidt, S.T. Nguyen and J.T. Hupp.; *Chem. Soc. Rev.* (2009)**38**, 1450–1459.
- [20] C. Zhang and L. Ai.; *J. Jiang, Ind. Eng. Chem. Res.* (2015)**54**, 153–163.
- [21] H. Li, Y. Zhou, W. Tu, J. Ye and Z. Zou.; *Adv. Funct. Mater.* (2015)**25**, 998–1013.
- [22] C. Wang, K.E. deKrafft and W. Lin.; *J. Am. Chem. Soc.* (2012) **134**, 7211–7214.
- [23] W. Zhu, P. Liu, S. Xiao, W. Wang, D. Zhang and H. Li.; *Appl. Catal. B: Environ.* (2015),**172–173**, 46–51.
- [24] P. Shukla, I. Fatimah, S. Wang, H.M. Ang, M.O. Tade, *Catal. Today* 157 (2010), 410–414.
- [25] H. Sun, S. Liu, S. Liu and S. Wang.; *Appl. Catal. B: Environ.*; (2014) **146**, 162–168.
- [26] L. Duan, B. Sun, M. Wei, S. Luo, F. Pan, A. Xu and X. Li.; *J. Hazard. Mater.*; (2015)**285**, 356–365.
- [27] J.J. Du, Y.P. Yuan, J.X. Sun, F.M. Peng, X. Jiang, L.G. Qiu, A.J. Xie, Y.H. Shen and J.F. Zhu.; *J. Hazard. Mater.*; (2011)**190**,945–951.
- [28] L. Ai, C. Zhang, L. Li and J. Jiang.; *Appl. Catal. B: Environ.* (2014)**148–149**, 191–200.
- [29] A. A. A. Emara , A. M. Taha, M. M. Mashaly and O. M. I. Adly.; *Eur. J. Chem.*, (2015)**6(2)**, 107-116
- [30] S. Cao, C.J. Wang, X.J. Lv, Y. Chen and W.F. Fu.; *Appl. Catal. B: Environ.* (2015)**162**, 381–391.

- [31] T. Baran, S. Wojtyła, A. Dibenedetto, M. Aresta and W. Macyk,; *Appl. Catal. B: Environ.* (2015) **178**, 170–176.
- [32] C.C. Wang, J.R. Li, X.L. Lv, Y.Q. Zhang and G. Guo, *Energy Environ. Sci.*; (2014) **7**, 2831–2867.
- [33] D. Wang, R. Huang, W. Liu, D. Sun and Z. Li,; *ACS Catal.*; (2014) **4**, 4254–4260.
- [34] M. M. Emar, N. H. Amin, S. M. K. AboulFotouh, M. M. EL-Moselhy and Mai S. Abd-El-Maqsoud, *Inter. J. Enviro.*; (2015) **4**, 322-335
- [35] J.P.S.Sousa, A.M.T.Silva, M.F.R.Pereira and, Figueiredo; *J.L. Science & Technology.* (2010) **45**, 1546–1554
- [36] B.Ohtani, O.O.Prieto-Mahaney, F.Amano, N.Murakami, and R. Abe, *J. Adv. Oxid. Technol.*; (2010) **13**, 247-253.
- [37] M. Misra, P. Kapur, and M. L. Singla. *Appl. Catal. B.* (2014) **605**, 150-151.